SLAC-PUB-2517
May 1980
(T/E)

TWO-PHOTON INTERACTIONS FROM MARK II AT SPEAR*

Robert Hollebeek
Stanford Linear Accelerator Center
Stanford University, Stanford, California 94305

Abstract: Results on the two-photon production of the η', f(1270), A_2(1310), and f'(1515) mesons at SPEAR energies are presented using data taken with the Mark II detector. The radiative width of the η' has been determined to be $\Gamma_{\gamma\gamma}(\eta') = 5.8 \pm 1.1$ keV (20% systematic uncertainty). Upper limits for the radiative widths of the f, A_2, and f' have been determined.

Résumé: Nous présentons des resultats sur la production de η', f(1270), A_2(1310) et f'(1515) aux energies de SPEAR par le procés de 2γ dans le detecteur Mark II. La largeur radiative de η' est determinée comme $\Gamma_{\gamma\gamma}(\eta') = 5.8 \pm 1.1$ keV (20% dérreurs systematiques). Des limites superieurs aux largeurs radiatives ont eté determinées pour les mesons f, A_2 et f'.

(Presented at the XVth Rencontre de Moriond: Electroweak Interactions and Unified Theory Predictions, Les Arcs, France, March 15-21, 1980.)

* Work supported by the Department of Energy under contract DE-AC03-76SF00515.

I. TWO PHOTON PHYSICS

The theory and phenomenology of the two-photon mechanism for the production of leptons and hadrons in electron-positron colliding beam experiments have been discussed extensively during the past ten years.[1] The lowest order single-photon process

$$e^+ + e^- \to \gamma^* \to X$$

produces neutral final states of charge conjugation C = – while the two-photon process

$$e^+ + e^- \to e^+ + e^- + \gamma^* + \gamma^* \to e^+ + e^- + X$$

produces neutral final states of charge conjugation C = +. The dominant diagram for this two-photon process is shown in Fig. 1. Despite the fact that this process is a higher order cross-section in QED, it is well known that the cross-section for fixed invariant mass of the two gamma system rises logarithmically with beam energy and becomes large at currently available energies. This behavior becomes evident when one writes down the cross section using the equivalent photon approximation which replaces the virtual photons with real bremsstrahlung photons radiated by the initial electron and positron. The cross section is then given by[2]

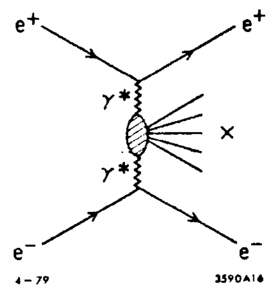

Fig. 1. Dominant diagram for the two photon production of state X.

$$\sigma_{e^+e^- \to e^+e^-X} \simeq 2\left(\frac{\alpha}{\pi}\right)^2 \left(\ell n \frac{E}{m_e}\right)^2 \int_{s_{threshold}}^{4E^2} \frac{ds}{s}\ \sigma_{\gamma\gamma\to X}(s)\ \ f(\sqrt{s}/2E)$$

where

$$f(x) = (2 + x^2)^2\ \ell n\,\frac{1}{x} - (1 - x^2)(3 + x^2)$$

If the system X is a C = + resonance, then the cross section can also be written using the radiative width of the resonance $\Gamma_{\gamma\gamma}$ as

$$\sigma_{e^+e^- \to e^+e^-R} \simeq \frac{16\alpha^2}{m_R^3}\left(\ell n\ \frac{E}{m_R}\right)^2\ \Gamma_{\gamma\gamma}\ \ (2J + 1)\ \ f(m_R/2E)$$

where J is the spin of the resonance. The asymptotic form of $f(m_R/2E)$ for large E is just $4\ \ell n\ (2E/m_R)$.

Even though this reaction has been discussed extensively, the amount of experimental information gathered has been quite limited until recently. Lepton pair production by this reaction was observed by several experiments[3-7] but only a few events with hadrons in the final state have been observed.[7-9] The first evidence for meson resonance production was reported by the SLAC-LBL Mark II collaboration[10] which observed the reaction

$$e^+e^- \rightarrow e^+e^-\eta'(958)$$

using the $\eta' \rightarrow \pi^+\pi^-\gamma$ final state.

The low mass C = + hadrons are shown in Table I together with their quark model assignments. Since the two-gamma cross section for meson production is proportional to the radiative width $\Gamma_{\gamma\gamma}$, these widths can be measured and compared to the theoretical values calculated from their quark constituents. This possibility was originally pointed out by F. Low[11] in 1960, who suggested that $e^+e^- \rightarrow e^+e^-\pi^o$ be used as a means of measuring the radiative width of the π^o meson.

TABLE I

$q\bar{q}$ State	C = + Mesons
^1S_o	π^o η $\eta'(958)$ η_c
$3P_o$	ε ε' S*(980)
$3P_1$	$A_1(1100)$ forbidden
$3P_2$	f(1270) f'(1515) $A_2(1310)$

In some cases one could hope to distinguish between quark models with fractional charge and those with integer charge since the radiative widths in these two models differ. In the case of the η' meson, for example, these widths differ by about a factor of four. The difference comes about because in the integer quark model the electromagnetic current has a color octet part in addition to the usual color singlet current.[12] Unfortunately, the predicted radiative widths of the mesons are sensitive to the transformation properties of their wave functions under color SU(3), and their quark composition. Meson states of u, d, and s quarks which are eigenstates corresponding to pure color octet and singlet are

$$(\bar{u}u - \bar{d}d)/\sqrt{2},\ (\bar{u}u + \bar{d}d - 2\bar{s}s)/\sqrt{6} \qquad \text{octet}$$

and

$$(\bar{u}u + \bar{d}d + \bar{s}s)/\sqrt{3} \qquad \text{singlet} \quad .$$

If the spatial wave functions of these states are identical ("nonet symmetry"), then the ratio of their widths is 3:1:8. On the other hand, if the states correspond to "ideal mixing," i.e. mixing of u and d quarks only, the states are

$$(\bar{u}u - \bar{d}d)/\sqrt{2},\quad (\bar{u}u + \bar{d}d)/\sqrt{2},\quad s\bar{s}$$

and again using nonet symmetry, the widths are in the ratio 9:25:2. In the case of the π^0, η and η' mesons, the usual assumptions are small octet singlet mixing and nonet symmetry and then the radiative width of the η' agrees well with the calculated value from the fractional charge model. In the integer charge model, the spatial wave function of the η' must be modified by a factor of 1/2 in violation of nonet symmetry to cancel the extra contribution from the color octet part of the current.

Before discussing high mass resonance production, it is useful to examine the dependence of the two photon cross section on the beam energy and the resonance mass. In the equivalent photon approximation, the flux of radiated photons is

$$N \approx \frac{2\alpha}{\pi}\left[\log\frac{E}{m_e} - 1/2\right]$$

when the scattered lepton is undetected. The cross section is found by integrating

$$\frac{N(\omega_1)\ N(\omega_2)}{\omega_1\ \omega_2}$$

$$N(\omega) \approx \frac{2\alpha}{\pi}\left[\frac{E^2 + (E-\omega)^2}{2E^2}\right]\ell n\left(\frac{E}{m_e} - 1/2\right)$$

where $s = m_R{}^2 = 4\omega_1\omega_2$. The photon flux at fixed $m_R{}^2$ together with $\frac{1}{\omega_1\omega_2}$ yields the factor

$$\frac{1}{m_R{}^2}\left(\ell n\,\frac{E}{m_e}\right)^2 f(\sqrt{s}/2E)$$

in the cross section. The $\gamma\gamma \rightarrow X$ cross section contributes a factor

$$s\sigma_{\gamma\gamma\rightarrow X} \sim (2J+1)\frac{\Gamma_{\gamma\gamma}}{m_R}$$

for a resonance and

$$s\sigma_{\gamma\gamma\rightarrow X} \sim (\ell n\ s/E^2)^n$$

for the continuum. This form gives

$$\sigma(M) \sim \frac{1}{M^2}\left(\ell n\,\frac{E}{m_e}\right)^2 \ell n\left(\frac{S}{M^2}\right)$$

if $n < 1$,[2] but the last logarithmic factor usually does not contribute to an increase in the experimentally observed yield since it is due to the logarithmic growth of the rapidity plateau for fixed M. Since most storage ring experiments have rather limited rapidity acceptances in the central detectors, the efficiency decreases like $1/\ln(s/M^2)$. For the resonance case,

$$\sigma(M) \sim \frac{1}{M^3} \ln\left(\frac{E}{m_e}\right)^2 (2J+1)\Gamma_{\gamma\gamma}$$

and there is a similar logarithmic variation of the efficiency. Although states in the 1 GeV mass range have now been observed at spear energies, the $1/M^3$ dependence of the resonance cross section makes the detection of high mass states like the η_c and η_b very difficult even for LEP energies.[13]

II. SEARCH FOR TWO PHOTON RESONANCE PRODUCTION WITH THE MARK II

The Mark II detector, shown in Fig. 2, has just been moved to PEP but has been running for the last year at SPEAR. The data taken at SPEAR have been used to search for the production of C = + resonances from the two-photon process. The performance of the detector has been discussed previously[10,14] and will not be elaborated on here. The technique used to find these resonant states is to search for various exclusive final states due to decay of the resonance. No tagging information is used since this would greatly reduce the efficiency for detection. Even without tagging, however, the one photon background coming from inclusive meson production with no other particles detected is small compared to the two photon production.

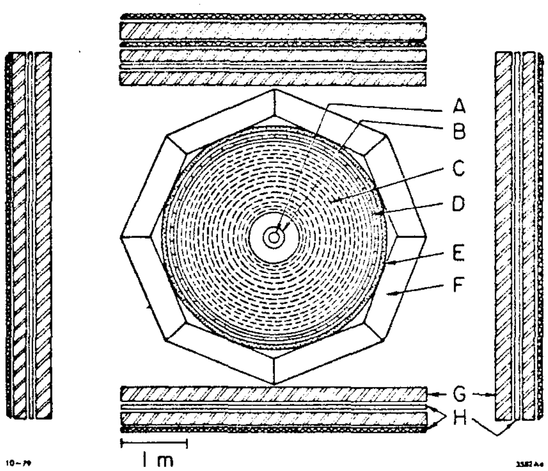

Fig. 2. Schematic view of the Mark II detector. (A) vacuum chamber, (B) pipe counter, (C) drift chambers, (D) time-of-flight counters, (E) magnet coil, (F) liquid argon shower counters, (G) iron absorber, and (H) muon proportional tubes.

The two photon total cross sections for π_o, η' and f production are each about 0.3 units of R at $E_{c.m.} = 6$ GeV with for example approximately 10% of the decays observable in the central detector in the case of the f meson. The kinematics of the two photon process, i.e. small transverse momentum of the meson with respect to the axis of the colliding beams, flat rapidity distribution, small visible energy, rising cross section, and coplanar two body decays can all be used to further reduce backgrounds and/or determine if the signal is due to the two photon process.

The final states which have been examined so far are shown in Table II. For the $\pi^+\pi^-\gamma$ final state, the pions are identified using the drift chambers (C), time of flight counters (D, Fig. 2), the liquid argon modules to reject electrons (F), and the muon chambers (H) to reject muons. Only those events with a $\pi^+\pi^-$ pair mass of less than 1 GeV/c^2 with each pion momentum less than 1 GeV/c were used. For the η' final state the photon energy is required to be within $0.180 < E_\gamma < 1.0$ GeV. For the f meson, the minimum photon energy in the $\pi\pi\gamma$ mode is increased to 0.250 GeV. Background from lepton or pion pairs produced by the two photon process combined with spurious noise counts in the liquid argon was eliminated by requiring that the transverse momentum of the $\pi^+\pi^-$ state be larger than 50 MeV/c and that the acoplanarity angle between the two pions be larger than 3°.[15] The resultant $\pi\pi\gamma$ mass spectrum is shown in Fig. 3a. Figure 3b shows the spectrum obtained by ignoring the measured gamma energy and using instead the energy obtained by constraining the $p_\perp$ of the $\pi\pi\gamma$ system to zero.

TABLE II

Meson	Final State
$\eta'(958)$	$\pi^+\pi^-\gamma$
f(1270)	$\pi^+\pi^-$
	K^+K^-
	$\pi^+\pi^-\gamma$
$A_2(1310)$	K^+K^-
	$\rho^\pm\pi$
f'(1515)	K^+K^-

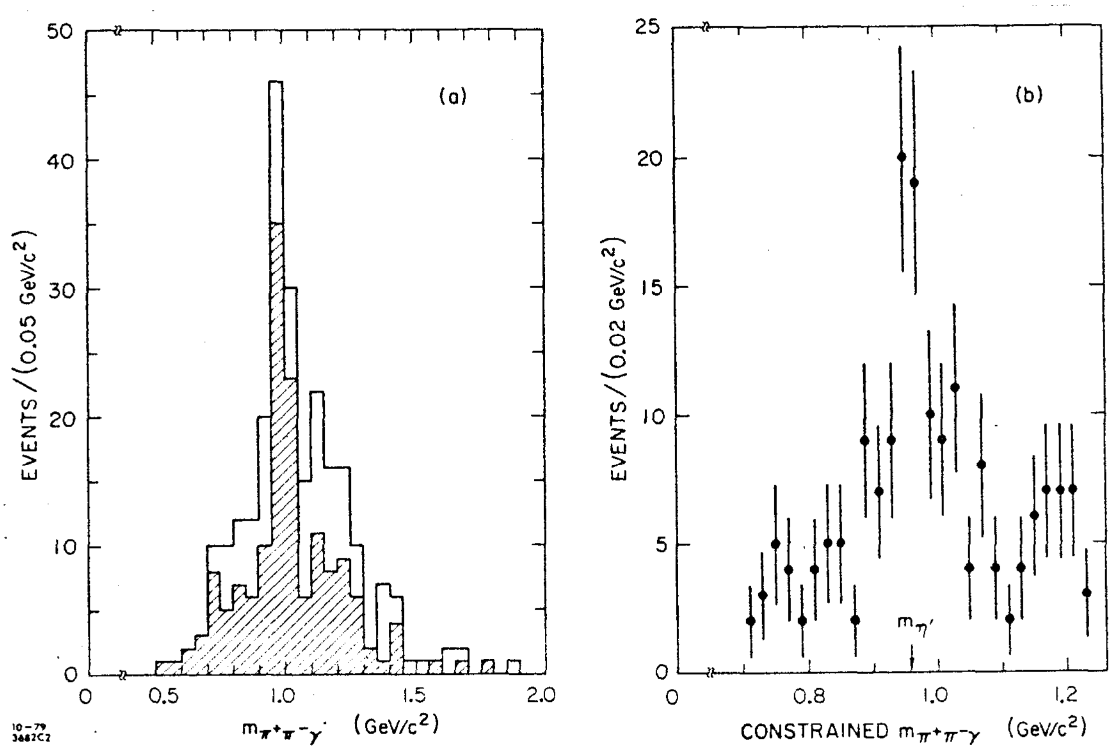

Fig. 3. (a) $\pi^+\pi^-\gamma$ invariant mass distribution. Shaded events are from $E_{beam} \geq 2.6$ GeV. (b) $\pi^+\pi^-\gamma$ invariant mass distribution with γ energy determined by $p_\perp = 0$ constraint.

A direct subtraction for background is made by using the adjacent mass bins in Fig. 3a and the cross section is calculated using the branching ratio $B(\eta' \to \pi^+\pi^-\gamma) = 0.298 \pm 0.017$.[16] The measured cross sections are shown in Table III and from them we determine $\Gamma_{\gamma\gamma}(\eta') = 5.8 \pm 1.1$ keV using the two-photon calculation of Ref. 17.

TABLE III

SUMMARY OF THE η' CROSS SECTION CALCULATION

E_b (GeV)	$\int\mathscr{L}dt$ (nb^{-1})	ε	$n_{\eta'}$	$\sigma(\eta')$ (nb)
1.95-2.21	4199	0.0231	7.7 ± 5.1	0.27 ± 0.18
2.25-2.50	2131	0.0224	4.3 ± 2.6	0.30 ± 0.18
2.50-3.00	6655	0.0211	25.9 ± 7.1	0.62 ± 0.17
3.00-3.35	4009	0.0177	20.0 ± 5.9	0.94 ± 0.28
3.70	984	0.0125	3.1 ± 2.2	0.84 ± 0.60

E_b is the beam energy, $\int\mathscr{L}dt$ is the integrated luminosity, ε is the detection efficiency not including $B(\eta' \to \pi\pi\gamma)$, $n_{\eta'}$ is the background subtracted number of η' events and $\sigma(\eta')$ is the observed cross section. Only statistical errors are shown.

To search for the f(1270) meson in the $\pi\pi\gamma$ channel, the same cuts were applied except that in order to decrease the background, the lower limit for the photon energy was increased to 250 MeV. The mass spectrum is shown in Fig. 4. The η' signal is reduced due to the photon energy cut and no f signal is seen. This allows us to set a 95% C.L. upper limit $\Gamma_{\gamma\gamma}(f)B(f \to \pi^+\pi^-\gamma) < 0.8$ keV. The luminosity weighted beam energy is 2.85 GeV.

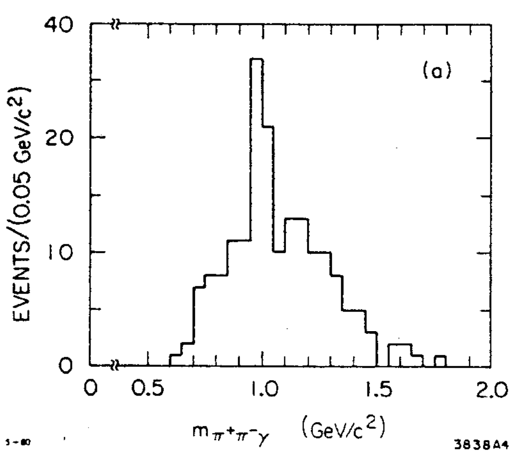

Fig. 4. $\pi^+\pi^-\gamma$ invariant mass distribution for $f(1270) \to \pi^+\pi^-\gamma$ search.

We have also looked for an A_2 signal in the $\rho^\pm\pi^\mp$ final state. Events with two photons and two oppositely charged tracks are selected. The invariant mass of the two photons is required to be within $0.075 < M_{\gamma\gamma} < 0.200$ GeV/c^2. The photon energies were then adjusted to constrain the invariant mass to the π^0 mass. These π^0 were combined with the $\pi^\pm$ to select events with a $\rho^\pm$ candidate defined as $0.5 < M_{\pi^\pm\pi^0} < 1.0$ GeV/c^2. The $\rho^\pm$ and $\pi^\mp$ momenta were required to be less than 800 MeV/c and the total final state transverse momentum was required to be less than 250 MeV/c. The detection efficiency for this final state is poor due to the low energy π^o efficiency. The upper limit for the cross section at E_b = 2.85 GeV is $\sigma(A_2) < 0.36$ nb and the upper limit for the radiative width is $\Gamma_{\gamma\gamma}(A_2) < 2.5$ keV.

The two body final states have very little one-photon contamination. Events are selected with two oppositely charged tracks whose acoplanarity angle is less than 20°. The $p_\perp$ of the final state is required to be less than 250 MeV/c. The invariant mass and $p_\perp$ distributions for the K^+K^- final state are shown in Figs. 5a and 5b. The kaon identification is achieved by requiring that each of the tracks have a larger than .65 probability to be a kaon as measured by the time-of-flight system. The f(1270), A_2(1310) and f'(1515) mesons are all expected to contribute to this final state. The statistics are too poor to allow a separation of these three states and only 95% C.L. upper limits have been determined. These limits are given in Table IV together with the limits on f production and A_2 production from the $\pi^+\pi^-\gamma$ and $\rho^\pm\pi^\mp$ channels respectively.

The analysis of the $\pi^+\pi^-$ final state is complicated by the fact that the detector does not unambiguously separate low momentum pions from the muons and electrons which are also produced by the two-photon process.

The time-of-flight system eliminates electrons below 300 MeV/c and the muon system eliminates muons above 700 MeV/c. The liquid argon system is used to eliminate electrons above about 500 MeV/c. The resulting

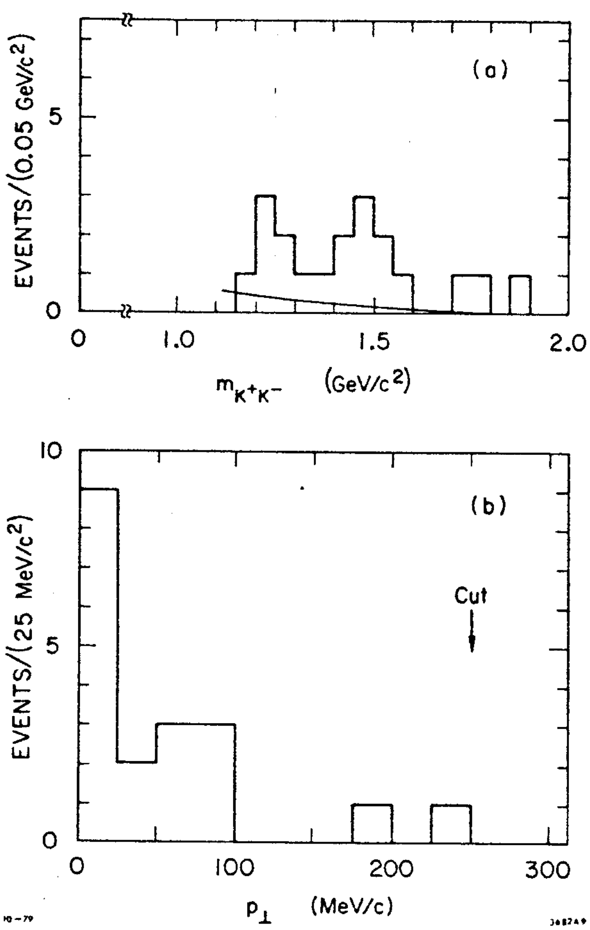

Fig. 5. (a) Invariant mass distribution for K^+K^- final state.
(b) Transverse momentum distribution of the K^+K^- system.

TABLE IV

Final State	Meson	ε	σ (nb)	$\Gamma_{\gamma\gamma}$ (keV)
$\pi^+\pi^-\gamma$	f(1270)	0.0200	$\sigma \times B(f \to \rho\gamma)$ < 0.14	$\Gamma_{\gamma\gamma} \times B(f \to \rho\gamma)$ < 0.8
$\rho^{\pm}\pi^{\mp}$	A_2(1310)	0.0028	< 0.36	< 0.25
K^+K^-	f(1270)	0.0167	< 4.2	< 24
K^+K^-	A_2(1310)	0.0172	< 2.6	< 17
K^+K^-	f'(1515)	0.0195	$\sigma \times B(f' \to K^+K^-)$ < 0.052	$\Gamma_{\gamma\gamma} \times B(f' \to K^+K^-)$ < 0.6

Upper limits (95% C.L.) on the two-photon production cross section σ and the radiative width $\Gamma_{\gamma\gamma}$ of the tensor mesons at the luminosity weighted average beam energy 2.85 GeV. The overall detection efficiency is listed under ε and B stands for branching ratio.

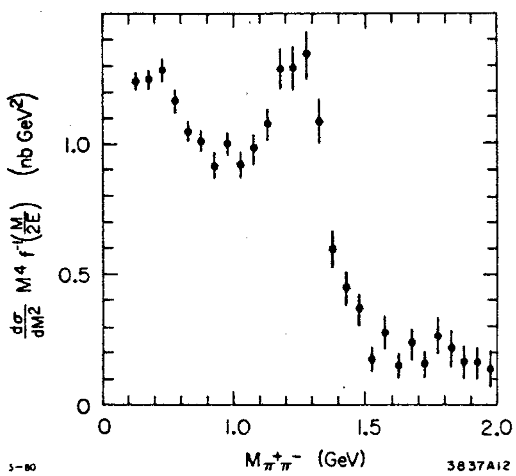

Fig. 6. $\pi^+\pi^-$ invariant mass distribution. Some contamination from two photon electron pair and muon pair final states remains.

invariant mass spectrum, assuming pion masses for both tracks, is shown in Fig. 6 and shows a clear f signal. The spectrum gives a poor chi-square when fit to a smooth background plus a Breit-Wigner line shape constrained to the mass and width of the f(1270). A final value for the radiative width of the f meson awaits an analysis of the feed-through of muons and electrons produced by the two-photon process and the possible contribution of the ε(1300) meson.

III. SUMMARY

A search has been made for the production of meson resonances produced by the two-photon process using the data taken by the Mark II collaboration at SPEAR. This process can be used to determine the radiative width of the observed mesons and these widths together with assumptions about the SU(3) properties of these mesons can provide tests of quark models. The η' in the $\pi^+\pi^-\gamma$ final state and the f meson in the $\pi^+\pi^-$ final have been observed and upper limits for the production of the f, A_2 and f' in several other final states have been determined. The radiative width of the η' is in good agreement with the predictions of quark models with fractionally charged quarks. The investigation of the C = + mesons produced by the two-photon process will be an important tool for determining the spectrum and properties of these states.

Acknowledgements

It is a pleasure to acknowledge the contributions of the MARK II collaboration to the collection and analysis of the data discussed in this talk. The author would also like to thank P. Jenni, D. Burke and F. Gilman for many useful discussions and suggestions.

References

1) For reviews of this subject and further references, see S. J. Brodsky, T. Kinoshita, and H. Terazawa, Phys. Rev. D4, 1532 (1971); H. Terazawa, Rev. Mod. Phys. 45, 615 (1973); V. M. Budnev et al., Phys. Reports 15C (1975).

2) S. J. Brodsky, T. Kinoshita, and H. Terazawa, Phys. Rev. D4, 1532 (1971).

3) V. E. Balakin, V. M. Budnev, and I. F. Ginsburg, Sov. Phys. JETP Lett. 11, 388 (1970).

4) V. E. Balakin et al., Phys. Lett. 34B, 663 (1971); C. Bacci et al., Nuovo Cimento Lett. 3, 709 (1972); G. Barbiellini et al., Phys. Rev. Lett. 32, 385 (1974).

5) A. Courau et al., Phys. Lett. 84B, 145 (1979).

6) H. J. Besch et al., Phys. Lett. 81B, 79 (1979).

7) R. Baldini Celio et al., Phys. Lett. 86B, 239 (1979).

8) S. Orito et al., Phys. Lett. 48B, 380 (1974); L. Paoluzi et al., Nuovo Cimento Lett. 10, 435 (1974).

9) Ch. Berger et al., Phys. Lett. 81B, 410 (1979).
Ch. Berger et al., DESY Report 79/65 (1979).

10) G. S. Abrams et al., Phys. Rev. Lett. 43, 477 (1979).

11) F. Low, Phys. Rev. 120, 582 (1960).

12) M. Chanowitz, Phys. Rev. Lett. 44, 59 (1980).

13) F. Gilman, SLAC PUB-2461, 1980.

14) W. Davies-White et al., Nucl. Instrum. Methods 160, 227 (1979).
G. S. Abrams et al., IEEE Trans. on Nucl. Sci. NS-25, 309 (1978).

15) These cuts are described in detail in Ref. 10.

16) Particle Data Compilation, Phys. Lett. 75B, 1 (1978).

17) V. M. Budnev and I. F. Ginzburg, Phys. Lett. 37B, 320 (1971);
V. N. Baier and V. S. Fadin, Nuovo Cimento Lett. 1, 481 (1971).